AIAA JOURNAL
Vol. 41, No. 3, March 2003

Acoustics and Thrust of Quiet Separate-Flow High-Bypass-Ratio Nozzles

Naseem H. Saiyed*
NASA John H. Glenn Research Center, Cleveland, Ohio 44135
Kevin L. Mikkelsen†
Aero Systems Engineering, St. Paul, Minnesota 55107
and
James E. Bridges*
NASA John H. Glenn Research Center, Cleveland, Ohio 44135

The NASA Glenn Research Center recently completed an experimental study to reduce the jet noise from modern turbofan engines. The study concentrated on exhaust nozzle designs for high-bypass-ratio engines. These designs modified the core and fan nozzles individually and simultaneously. In comparison with chevrons, tabs appeared to be an inefficient method for reducing jet noise. Data trends show that interaction between fan flow and the core cowl could strongly impact noise and cruise performance irrespective of the mixing device installed. The study demonstrates that modifications of the core nozzle are generally more advantageous than of the fan nozzle. Even greater advantage in noise reduction and associated cruise thrust penalties is demonstrated through simultaneous modification of both nozzles. The best nozzle design had a 0.06% cruise thrust loss and, corrected for takeoff thrust loss, a 2.7-EPNdB reduction for the effective perceived noise level metric. This design simultaneously employed chevrons on the core and fan nozzles. Last, five nozzle configurations with cruise thrust loss of less than 0.5% and noise reductions of over 2.5 EPNdB are identified as candidates for full-scale engine and flight demonstrations.

Nomenclature

C	=	speed of sound
C_{Tr}	=	nozzle thrust coefficient
c_p	=	pressure coefficient
F	=	thrust
$\dot{m}$	=	flow rate
P	=	pressure
q	=	tunnel dynamic pressure
V	=	velocity
Z	=	ratio of actual thrust to ideal thrust if sonic

Subscripts

a	=	ambient
c	=	core
d	=	experimental data
f	=	fan
g	=	gross
i	=	ideal
s	=	static

Introduction

THE impetus for this study was the increasingly stringent noise regulations designed to protect the communities around airports from aircraft noise pollution. Jet exhaust is one of the dominant noise sources from modern turbofan engines,[1] its dominance dramatically increasing with throttle push. These engines use two nozzles (Fig. 1) to separately exhaust flow from the core and fan, hence the name separate-flow nozzles (SFN). Mixing these two flows into a single flow prior to exhausting provides a thrust benefit relative to two separate flows.[2] However, integration factors associated with mixing the two flows (for example, extra nacelle weight, drag and thrust reverser complexity) negate the thrust benefits for high-bypass-ratio engines.

The NASA Glenn Research Center (GRC) recently completed an exhaustive experimental study to evaluate the jet noise from 54 SFN designs. This study, the separate-flow nozzle test (SFNT), was part of NASA's Advanced Subsonic Technology program and was a team effort between GRC, NASA Langley, Pratt and Whitney, United Technologies Research Corp., Boeing, General Electric, Allison, and Aero Systems Engineering (ASE). SFNT quantified the effects of bypass ratios, internal vs external plugs, core jet shielding, mixing of core and fan jets on far-field acoustics, plume profile, and thrust.

SFNT was conducted in two separate sequential investigations: acoustics phase and thrust phase. Acoustics phase included far-field acoustics, plume schlieren images, exhaust plume pressures and temperatures, plume infrared signatures and jet noise source locations using phased arrays. Data from this phase and processing details are provided in Refs. 3 and 4.

Data from the acoustics phase were also used to screen for the quiet SFN configurations as candidates for the thrust phase. Fourteen SFNs were chosen for this phase (13 test SFNs and one baseline SFN). Their bypass ratio of five represented majority of the current fleet. These SFNs attempted to reduce the fully expanded jet velocity by mixing 1) core flow with fan flow only, 2) fan flow with ambient flow only, or 3), 1 and 2 simultaneously. Based on the type of flow mixing attempted, these designs fell into two broad categories: tabs and chevrons. Very aggressive mixing characterized the tabs and very gently, the chevrons.

Takeoff thrust performance was evaluated on nine of the 14 SFNs as a result of funding limitations. Cruise thrust performance was evaluated for all 14 SFNs. This report summarizes the thrust phase findings and their application to the data from the acoustics phase.

Objectives

In this report the ideal effective perceived noise level (EPNL) values[5] are corrected for takeoff thrust performance. The cruise thrust data are examined to determine the effect of specific SFN design parameters on cruise thrust performance. SFN candidates for further development via static engine tests and flight tests for possible implementation in commercial service are recommended.

Received 20 November 2001; revision received 22 July 2002; accepted for publication 25 July 2002.

*Aerospace Engineer, Acoustics Branch, Structures and Acoustics Division. Member AIAA.
†Mechanical Engineer, Aerosystems Engineering, 358 Fillmore Avenue East. Member AIAA.

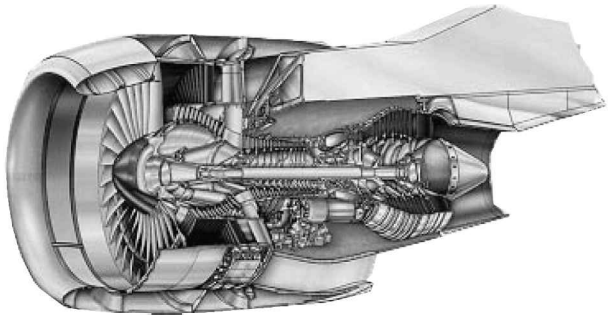

Fig. 1 Typical high-bypass-ratio, separate flow engine.

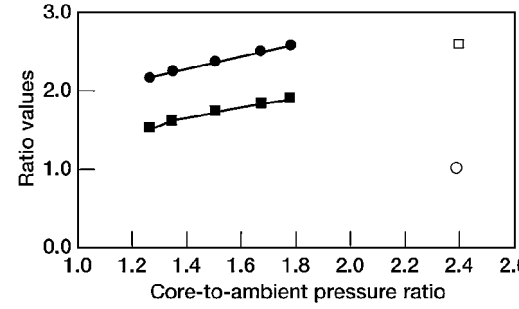

Fig. 2 Cycle points for acoustic and thrust performance tests: □, fan-to-ambient pressure ratio; ○, core-to-fan temperature ratio; ●, takeoff cycle; and ■, cruise.

Acoustic Tests at the NASA Glenn Research Center

The model scale acoustic data were collected on 54 SFN configurations, most of bypass ratio five. These data were scaled to an engine having nominal gross thrust of 50,000 lbf (222,000 N). The scale factor was eight. Spectra acquired at 0.28 M at a nominal radius of 50 ft (15.24 m) were processed to yield 1500-ft (457.2-m)-altitude 0.28 Mach level fly-over EPNLs. No ground corrections were applied because only relative EPNLs were desired. Single engine operation was assumed, and airframe effects were neglected. Hardware and test data details including plume surveys and computational fluid dynamic predictions are provided in Refs. 3 and 4. The 54 SFNs were reduced to 13 test SFNs for thrust performance tests, data used for this paper. This selection was based on the EPNL metric and SFN geometric variations.

Thrust Performance Tests at the ASE's FluiDyne Lab

Figure 2 shows the takeoff and cruise cycle points for the thrust performance tests. Unlike acoustic tests, these tests were run cold because these flows did not mix within a mixing chamber. Consequently, the temperature of unmixed flows had no impact on C_{Tr}:

$$C_{\mathrm{Tr}} = F_{g,d}/F_{g,i}$$

with $F_{g,i}$ calculated from

$$F_{g,i} = \dot{m}_c V_{c,i} + \dot{m}_f V_{f,i}$$

Therefore, C_{Tr} values from cold thrust performance tests would be identical to C_{Tr} values from hot thrust performance tests. Also, cold performance tests provide a stable model free of thermal expansion and heat transfer between the ducts. ASE's FluiDyne Aerotest Laboratory quotes the accuracy to be $\pm 0.25\%$ for absolute values of C_{Tr} at simulated flight.

The takeoff thrust performance data were acquired statically ($M = 0.0$) and at simulated flight ($M = 0.28$). Static data were acquired for SFN configurations in which only the core nozzle was modified because it was believed that the fan flow isolates the core shear layer from the ambient flow. Simulated flight data were acquired for SFN configurations in which the fan nozzle was modified (either individually or simultaneously with the core nozzle). The cruise thrust performance data were acquired at 0.8 Mach for all SFN configurations.

Hardware

The 13 test SFNs selected from acoustic tests employed tabs and chevrons. Following is a brief description of their major characteristics with specific details given in Refs. 3 and 4. Figure 3 shows the baseline SFN (also known as 3BB). The SFN hardware designation is 3-X_a-Y_b, where 3 is the model number, X is the core nozzle designation, Y is the fan nozzle designation, and subscripts a and b refer to the number of tabs or chevrons on each nozzle. For example, $3T_{48}C_{24}$ (B for baseline, C for chevrons, T for tabs, I for inward, and A for alternating) signifies that model 3 has a core nozzle with 48 tabs and a fan nozzle with 24 chevrons. All nozzles were convergent.

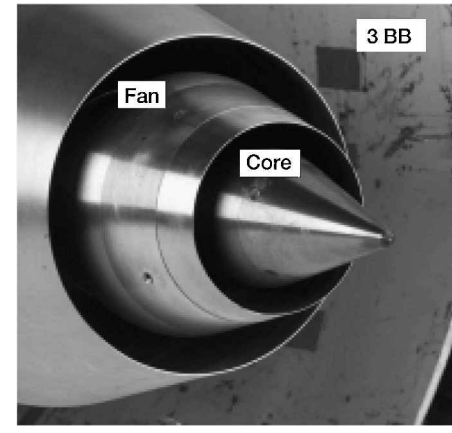

Fig. 3 Typical high-bypass-ratio, separate-flow nozzles: area of fan A_{fan}, 28.9 in.^{2} (186.45 cm^2) and area of core A_{core}, 10.5 in.^{2} (67.74 cm^2).

Tabs: Core Nozzle

Delta tabs were used to produce strong streamwise vortices to mix the core flow with the fan flow aggressively. Some tabs protruded into the core flow and some into the fan flow. The tab protrusion angle was 30 deg with respect to the core streamlines.[6] Some tabs did not protrude into either flow, that is, they remained neutral with a protrusion angle of 0 deg. Figure 4 shows two core nozzle tab configurations ($3T_{24}B$ and $3T_{48}B$). The six tabs protruding into the core flow for $3T_{24}B$ blocked 2.9% of the core geometric throat area. The 12 tabs protruding into the core flow for $3T_{48}B$ blocked 1.45% of the core geometric throat area.

Tabs: Fan Nozzle

To mix the fan flow with the ambient flow aggressively, delta tabs were used to produce strong streamwise vortices. Some tabs protruded into the fan flow and some into the ambient flow. The tab protrusion angle was 30 deg with respect to the fan streamlines.[6] Some tabs did not protrude into either flow but remained neutral with a protrusion angle of 0 deg. Figure 5 shows tabs on fan nozzle configuration $3BT_{48}$. The 12 tabs protruding into the fan flow blocked about 2% of the fan geometric throat area.

Chevrons: Core Nozzle

Chevrons are serrations on the nozzle exit plane for creating streamwise vortices, albeit much more gently than the delta tabs do. Figure 6 shows three configurations with 12 chevrons each ($3C_{12}B$, $3I_{12}B$, and $3A_{12}B$). The $3C_{12}B$ configuration has simple serrations on the nozzle exit plane; these remain parallel with core streamlines. Chevrons from the $3I_{12}B$ configuration protruded into the core flow only about one displacement thickness of the core boundary layer. They inclined about 3 deg with respect to core streamlines, a very gradual inclination. Chevrons from the $3A_{12}B$ configuration protruded into both the core flow and the fan flow. They also gradually inclined about 3 deg with respect to core streamlines.

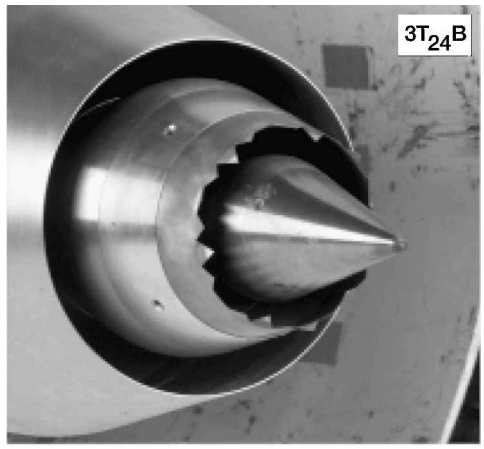

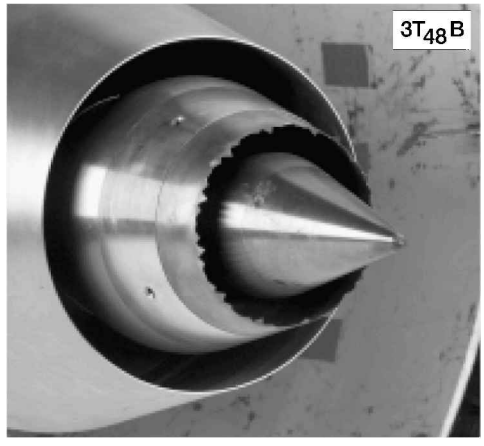

Fig. 4 Tabs on core nozzle only.

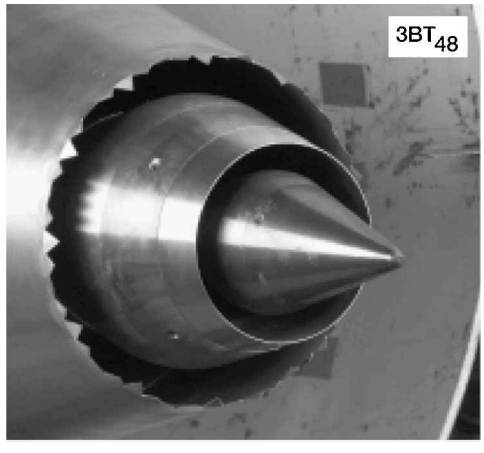

Fig. 5 Tabs on fan nozzle only.

Chevrons: Fan Nozzle

Figure 7 shows fan chevron configuration $3BC_{24}$. The 24 chevrons were simple serrations on the nozzle exit plane and remained parallel with fan streamlines.

Core and Fan Nozzles: Simultaneously

The hardware in the configurations described thus far modified the core and fan nozzles individually. Both nozzles were modified simultaneously for six tests. Figure 8 shows these six combinations: $3T_{24}T_{48}$, $3T_{48}T_{48}$, $3T_{48}C_{24}$, $3I_{12}C_{24}$, $3A_{12}C_{24}$, and $3T_{24}C_{24}$.

Facilities

The acoustic tests were conducted in the NASA Glenn Aeroacoustic Propulsion Laboratory (AAPL), a 65-ft (19.8-m)-radius geodesic dome (Fig. 9). Castner[7] and Cooper[8] give additional details about

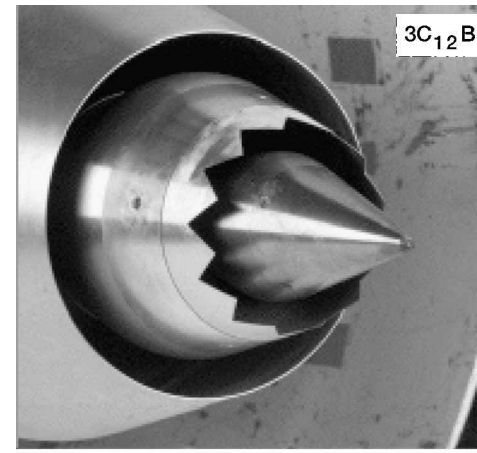

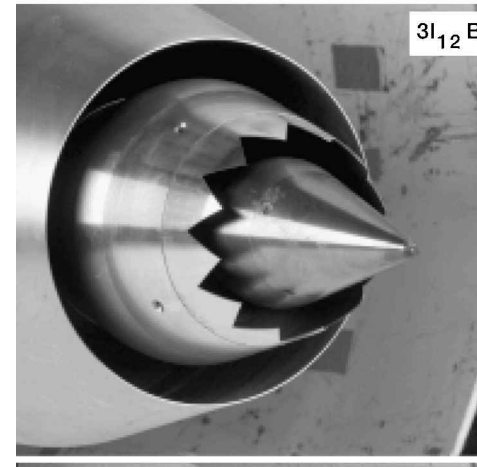

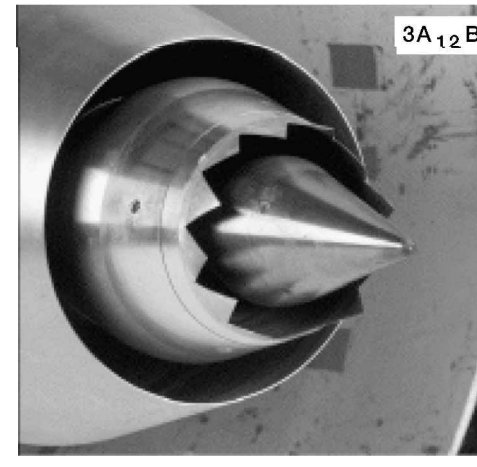

Fig. 6 Chevrons on core nozzle only.

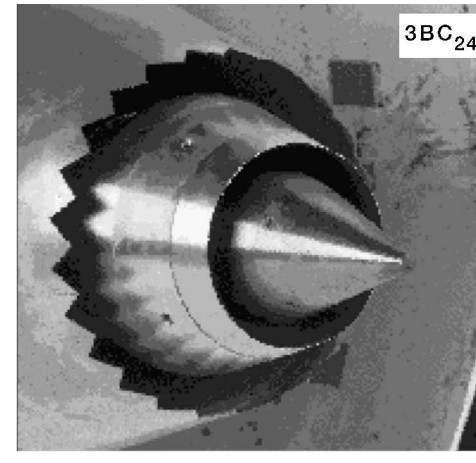

Fig. 7 Chevrons on fan nozzle only.

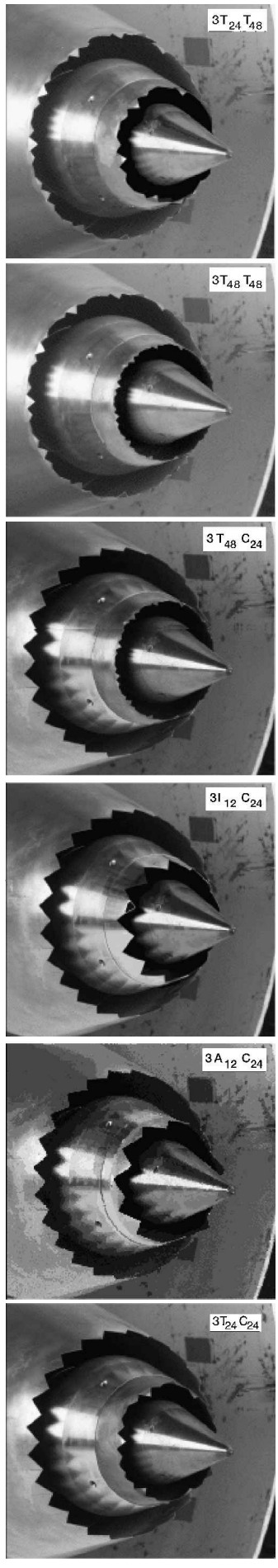

Fig. 8 Core and fan modifications simultaneously.

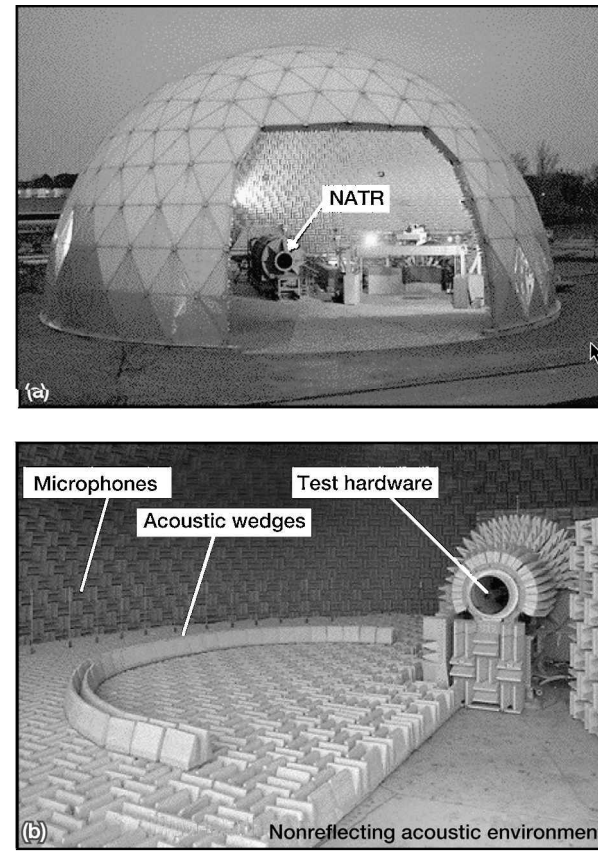

Fig. 9 Aeroacoustic Propulsion Laboratory: a) outside and b) inside.

the dome. Since Cooper's report, the concrete floor of the AAPL was covered with 2-ft (0.61-m)-high acoustic wedges to upgrade the facility to fully anechoic status. Located inside and at the center 10 ft (3.05 m) above the concrete floor is the jet exit rig, which simulates hot engine flows and to which the test articles are attached. A 53-in. (134.6-cm)-diamduct (freejet) surrounds the rig and provides the air to simulate flight on the rig and on the test article. The freejet and the jet exit rig comprise the Nozzle Acoustic Test Rig. A set of 0.25-in. (6.35-mm) microphones (26 total) located 10 ft (3.05 m) above the concrete floor surround the rig from 40 deg (forward arc) to 165 deg (aft arc) in 5-deg increments. The microphones are located at a nominal radius of 50 ft (15.24 m) from the test article. The performance tests were conducted at ASE's FluiDyne Aerotest Laboratory. Static and simulated flight test setups are shown in Figs. 10a and 10b, respectively.

Experimental Results

This section presents the results of correcting the ideal acoustic performance of 14 SFNs (based on the EPNL metric) for takeoff thrust performance and the effects of SFN design parameters on cruise performance. Suggestions are made regarding further development of candidate SFNs for future implementation into service.

Thrust-Corrected EPNLs

The thrust performance data were acquired at the same pressure ratios as the acoustics data, that is, the takeoff power cycle. Dependence of C_{Tr} on ideal gross thrust was determined for all nine SFNs (eight test SFNs and 3BB SFN) using these data. This dependence was evaluated at $F_{g,i}$ for determining $F_{g,d}$.

Day-to-day changes in ambient conditions slightly alter $F_{g,i}$. All EPNL data are corrected by normalizing $F_{g,i}$ against a reference thrust of 100 lbf (445 N), which ensures that variations in EPNL are from SFN designs and not from small variations in $F_{g,i}$.

The normalized EPNLs are plotted against the fully mixed jet velocity V_{mix} normalized with the ambient speed of sound c_{amb}:

$$Z = V_{\mathrm{mix}}/c_a$$

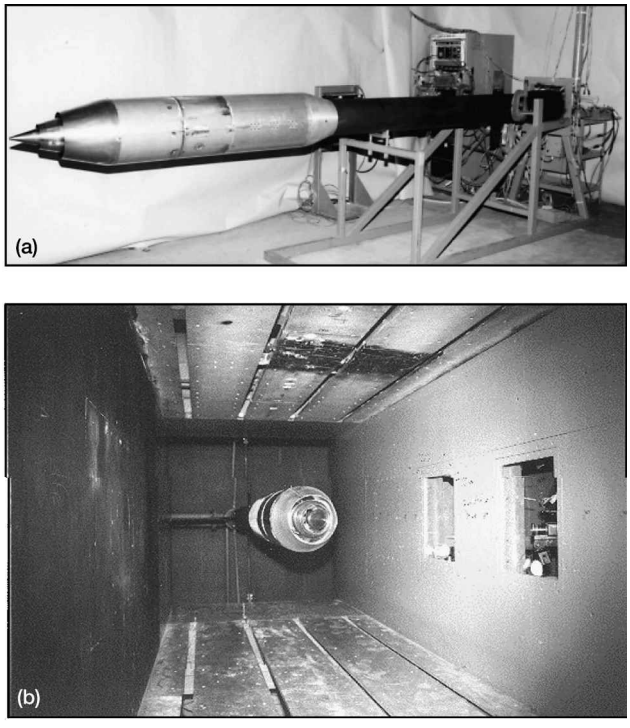

Fig. 10 Thrust stands at Aero Systems Engineering FluiDyne Aerotest Group: a) static and b) flight.

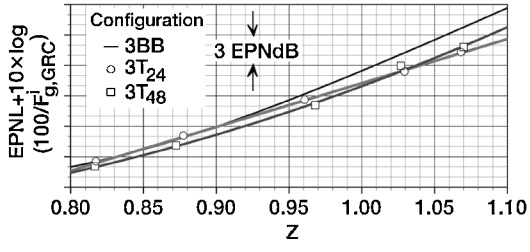

Fig. 11 Effective perceived noise level benefits with tabs on core nozzle.

where V_{mix} is calculated from

$$V_{\text{mix}} = F_{g,d}/(\dot{m}_c + \dot{m}_f)$$

Acoustic Performance

Acoustic tests of the 3BB SFN were repeated several times during the SFNT. Plotting these data as EPNL vs Z collapsed over 90% of the data within ±0.5 EPNdB (Refs. 3 and 4); therefore, these data are represented by a curve fit (regression coefficient R^2 of 0.995) rather than by symbols to avoid data clutter. Also, the value of 1.07 for Z, representing the average growth gross takeoff thrust, was selected for evaluating the EPNL values.

Tabs: Core Nozzle

Figure 11 presents an EPNL plot for two SFNs with core tabs ($3T_{24}B$ and $3T_{48}B$). The EPNL reduction, relative to 3BB, appears to be a function of both tab size and thrust. The $3T_{48}B$ EPNL reduction becomes constant at 1.9 EPNdB beyond $Z = 1.05$. The $3T_{24}B$ reductions, however, appear to increase continually with thrust, providing about 2.5 EPNdB at $Z = 1.07$. EPNL reductions seem to grow with tab size at high thrust values, and the trend is reversed at very low thrust values.

Chevrons: Core Nozzle

Figure 12 presents EPNL plots for two core chevrons and again shows a dependence of EPNL reduction on thrust. The $3I_{12}B$ SFN provided 2.1-EPNdB reduction, which is significantly better than that obtained from $3C_{12}B$ at 1.2 EPNdB. The obvious difference between these two configurations is that the $3I_{12}B$ SFN penetrated the boundary layer and $3C_{12}B$ SFN remained parallel with the core

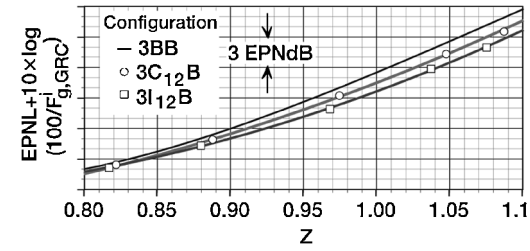

Fig. 12 Effective perceived noise level benefits with chevrons on core nozzle.

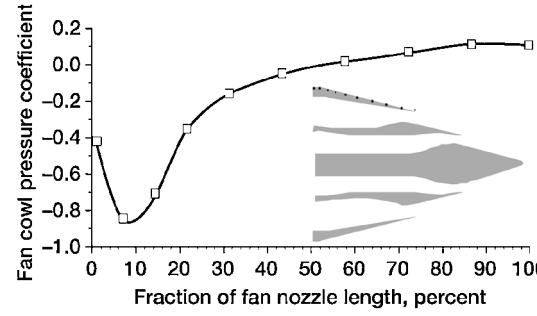

Fig. 13 Static-pressure distribution on fan cowl at Mach 0.8.

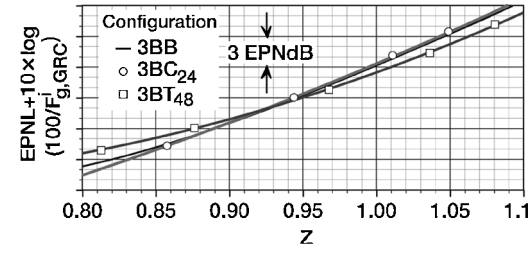

Fig. 14 Effective perceived noise level benefits with tabs and chevrons on fan nozzle.

streamlines. It seems that some boundary-layer penetration, however small, is needed for greater noise reduction.

Tabs and Chevrons: Fan Nozzle

The fan nozzle boattail angle was 14 deg. This high value was needed to ensure that NASA Glenn's baseline acoustic data could be compared with similar data planned for NASA Langley's Jet Noise Laboratory. Also, this value was a compromise among various nacelles to avoid tests of company specific nacelle geometries.

Figure 13 shows the fan cowl pressure coefficient at 0.8 Mach calculated from

$$c_p = (P_{s,\text{surface}} - P_{s,\text{tunnel}})/q$$

All static ports were flush with the surface except for the last port, where the nozzle lip was too thin. Instead, tubing was attached to the nozzle surface, its opening flush with the nozzle base. The flow rapidly expands around the fan shoulder. Such high expansion is reasonable given that the afterbody was not tapered in these tests.[9–13] There was no clear evidence of shocks and flow separation, and the expansion appears to recover smoothly. Slight overcompression is seen in the last half of the nozzle.

Figure 14 presents an EPNL plot for fan chevrons ($3BC_{24}$) and fan tabs ($3BT_{48}$). Apparently, the $3BC_{24}$ SFN was 0.2 EPNdB louder than 3BB. Tabs on the fan nozzle ($3BT_{48}$), however, provided about 1.1 EPNdB reduction with respect to 3BB SFN at $Z = 1.07$ but an increase of about 1.0 EPNdB at low thrust ($Z = 0.85$). At low thrust the 48 tabs simply could not entrain air to slow the jet exhaust enough to cause a significant reduction in low-frequency jet noise; in fact, the attempt to do so created high-frequency noise.[4]

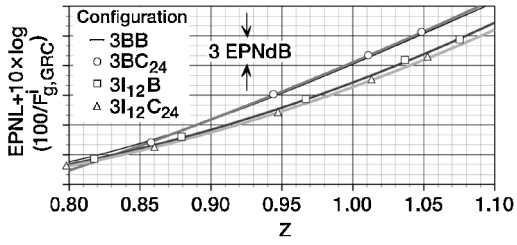

Fig. 15 Effective perceived noise level benefits with chevrons on core and nozzles simultaneously.

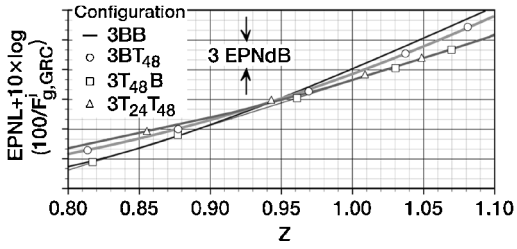

Fig. 16 Effective perceived noise level benefits with tabs on core and nozzles simultaneously.

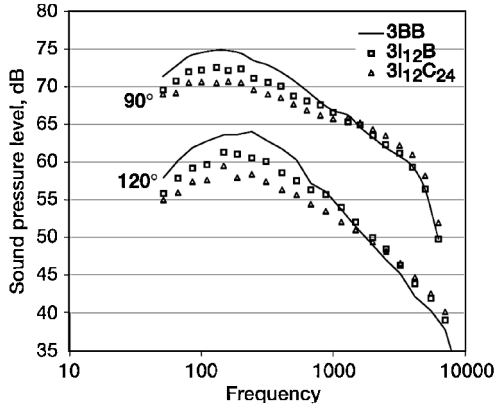

Fig. 17 Jet noise fly-over spectra.

Core Chevrons with Fan Chevrons: Simultaneously

The EPNL reductions from individually modified core nozzles and fan nozzles were presented in the preceding sections. The results of modifying these nozzles simultaneously are now presented. Figure 15 compares the EPNLs from an SFN simultaneously using chevrons on core and fan nozzles ($3I_{12}C_{24}$) with 3BB. A reduction of about 2.7 EPNdB is seen at $Z = 1.07$ and seems to remain constant beyond high thrusts.

This figure also compares $3I_{12}C_{24}$ data with that for $3I_{12}B$ and $3BC_{24}$. Adding chevrons to the fan nozzle increased the EPNL reduction demonstrated from $3I_{12}B$ SFN by 0.6 EPNdB (from 2.1–2.7 EPNdB).

Core Tabs with Fan Tabs: Simultaneously

Figure 16 compares the EPNLs from an SFN simultaneously using tabs on the core and fan nozzles ($3T_{24}T_{48}$) with 3BB. The EPNL reduction of about 2.4 EPNdB is seen at growth gross takeoff thrust and seems to continually increase with thrust.

Figure 16 also compares $3T_{24}T_{48}$ data with that from $3T_{24}B$ and $3BT_{48}$. Tabs alone on the fan nozzle had created such intense excess mixing noise at low thrust ($Z = 0.85$) that the EPNL increased by 1 EPNdB relative to 3BB. Combining core and fan tabs exacerbated the mixing noise for a total EPNL increase of 1.4 EPNdB relative to 3BB at $0.85Z$.

Acoustic Details

Figure 17 compares the far-field spectra at 90 and 120 deg with respect to the inlet for two chevron SFNs at 1500-ft altitude. Substantial reductions are seen in low frequency with little gain in the excess noise at high frequencies.

Cruise Performance and Engine SFN Downselect

Figure 18 shows C_{Tr} losses and EPNL reductions from 13 SFNs relative to the baseline, the 3BB. All cruise data were taken at Mach 0.8. Changes in C_{Tr} values relative to 3BB are shown as ΔC_{Tr}. The units of ΔC_{Tr} are in percent relative to C_{Tr}. For example, the ΔC_{Tr} for a nozzle with a C_{Tr} value of 0.98 is 2.0% relative to an ideal nozzle with a C_{Tr} value of 1.0.

Fan chevrons were tested with four core nozzle mixing devices ($3I_{12}C_{24}$, $3A_{12}C_{24}$, $3T_{24}C_{24}$, and $3T_{48}C_{24}$). In all but $3A_{12}C_{24}$, the fan chevrons reduced the SFN thrust loss relative to when baseline fan nozzle was used with four core nozzle mixing devices ($3I_{12}B$, $3A_{12}B$, $3T_{24}B$, and $3T_{48}B$).

Fan tabs were tested with two core nozzle tab designs ($3T_{24}T_{48}$ and $3T_{48}T_{48}$). In both cases the fan tabs increased the SFN thrust loss relative to when baseline fan nozzle was used with two core

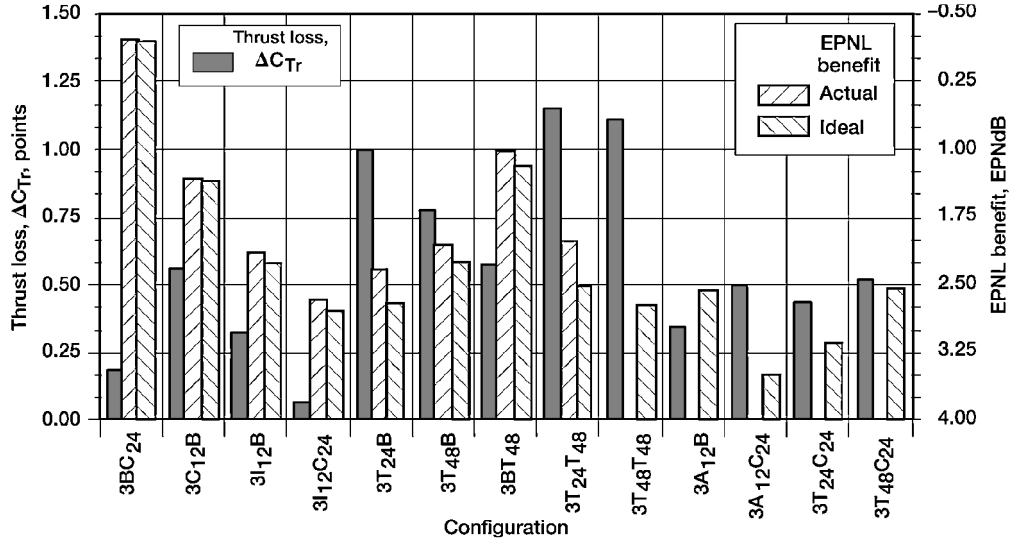

Fig. 18 Effective perceived noise level and cruise thrust losses relative to 3BB.

Table 1 EPNL reductions and cruise losses

SFN configuration	EPNL reduction, EPNdB		Cruise thrust loss, ΔC_{Tr}, %
	Ideal	Actual	
3BB	Baseline	Baseline	Baseline
$3BC_{24}$	−0.16	−0.1	0.18
$3C_{12}B$	1.38	1.3	0.55
$3I_{12}B$	2.29	2.1	0.32
$3I_{12}C_{24}$	2.82	2.7	0.06
$3T_{24}B$	2.73	2.3	0.99
$3T_{48}B$	2.29	2.0	0.77
$3BT_{48}$	1.22	1.0	0.57
$3T_{24}T_{48}$	2.56	2.0	1.14
$3T_{48}T_{48}$	2.77	——	1.10
$3A_{12}B$	2.59	——	0.34
$3A_{12}C_{24}$	3.52	——	0.49
$3T_{24}C_{24}$	3.16	——	0.43
$3T_{48}C_{24}$	2.58	——	0.51

nozzle tab designs ($3T_{24}B$ and $3T_{48}B$). Increase was not linear, that is, $3T_{24}B$'s loss of 0.99% and $3BT_{48}$'s loss of 0.57% did not add to $3T_{24}T_{48}$'s loss of 1.14%. Also, doubling the tab numbers on the core nozzle did not double its loss perhaps because of expansion losses on the core cowl and the plug.

This figure shows the ideal EPNL reductions for all configurations. But the thrust-corrected EPNL reductions (actual EPNL reductions) are shown only for the first eight SFNs ($3BC_{24}$ to $3T_{24}T_{48}$). It appears that nozzle designs having cruise thrust losses of up to 0.5% are efficient enough during takeoff to maintain the actual EPNL reductions close to ideal EPNL reductions.

Jet noise reduction without thrust loss is a very challenging requirement. The constraints of a particular application dictate the jet noise reduction needed and the tolerable thrust loss. For this generic document these limits are set as 1) a maximum cruise thrust loss of 0.5% and 2) a minimum EPNL reduction of 2.5 EPNdB. Although no cruise thrust loss is desirable, SFNs with C_{Tr} losses above 0.5% are likely to be extremely unfavorable. Jet noise reductions less than 2.5 EPNdB are likely to have a much smaller effect on the airplane total EPNL reductions. A particular application will dictate these limits; however, 0.5% and 2.5-EPNdB limits provide a starting place. Five SFNs met this metric: $3I_{12}C_{24}$, $3T_{24}C_{24}$, $3A_{12}C_{24}$, $3A_{12}B$, and $3T_{48}C_{24}$. They should be considered as candidates for further development and verification via static engine tests and flight tests. Table 1 summarizes the noise reductions and thrust penalties for all configurations.

Summary

NASA Glenn Research Center recently completed an extensive experimental study to reduce jet noise. The study concentrated on exhaust nozzle designs for high-bypass-ratio engines. A total of 54 SFNs were tested by modifying the core nozzle alone, the fan nozzle alone, or both nozzles simultaneously.

Noise reductions were achieved from both chevrons and tabs. EPNL reductions seemed to increase with tab size at high thrust values, with the trend reversing at very low thrust values. Chevrons need to gently penetrate the boundary layer, albeit a small amount, for substantial noise reduction.

Simultaneous application of fan devices with core devices is advantageous for reductions in both takeoff noise and associated cruise thrust penalties. Fan chevrons tend to reduce the cruise thrust loss when used with core chevrons or tabs. Fan tabs tend to increase the cruise thrust loss when used with core tabs. Neither chevrons nor tabs were as effective on the fan nozzle as they were on the core nozzle.

A metric was selected to find the suitable SFNs for further development and verification via static engine tests and flight tests. The metric was the maximum C_{Tr} loss of 0.5% and the minimum EPNL reduction of 2.5 EPNdB. Five SFNs that achieved the metric and therefore should be considered for further development are $3I_{12}C_{24}$, $3T_{24}C_{24}$, $3A_{12}C_{24}$, $3A_{12}B$, and $3T_{48}C_{24}$.

References

[1]Groeneweg, J. F., and Rice, E. J., "Aircraft Turbofan Noise," *Journal of Turbomachinery*, Vol. 109, Jan. 1987, pp.130–141.

[2]Kerrebrock, J. L., *Aircraft Engines and Gas Turbines*, 2nd ed., MIT Press, Cambridge, MA, 1992, pp. 1–50.

[3]Janardan, B. A., Hoff, G. E., Barter, J. W., Martens, S., Gliebe, P. R., Mengle, V., and Dalton, W. N., "AST Critical Propulsion and Noise Reduction Technologies for Future Commercial Subsonic Engines: Separate-Flow Exhaust System Noise Reduction Concept Evaluation," NASA CR-2000-210039, Dec. 2000.

[4]Low, John K. C., Schweiger, Paul S., and Premo, J. W., "Advanced Subsonic Technology (AST) Separate-Flow High-Bypass Ratio Nozzle Noise Reduction Program Test Report," NASA CR-2000-210040, Dec. 2000.

[5]Smith, M. J. T., *Aircraft Noise*, Cambridge Univ. Press, Cambridge, MA, 1989, pp. 150–200.

[6]Zaman, K. B. M. Q., Reeder, M. F., and Samimy, M., "Control of an Axisymmetric Jet Using Vortex Generators," *Physics of Fluids*, Vol. 6, No. 2, 1994, pp. 778–793.

[7]Castner, R. S., "The Nozzle Acoustic Test Rig: An Acoustic and Aerodynamic Free-Jet Facility," NASA TM-106495, April 1994.

[8]Cooper, B. A., "A Large Hemi-Anechoic Enclosure for Community-Compatible Aeroacoustic Testing of Aircraft Propulsion Systems," NASA TM-106015, April 1993.

[9]Blaha, B. J., Chamberlin, R., and Bober, L. J., "Boundary Layer Thickness Effect on Boattail Drag," NASA TMX-73443, Jan. 1976.

[10]Chamberlin, R., "Flight Investigation of 24° Boattail Nozzle Drag at Varying Subsonic Flight Conditions," NASA TMX-2626, Nov. 1972.

[11]Wing, D. J., "Afterbody/Nozzle Pressure Distributions of a Twin-Tail Twin-Engine Fighter with Axisymmetric Nozzles at Mach Numbers from 0.6 to 1.2," NASA TP-3509, May 1995.

[12]Wing, D. J., "Performance Characteristics of Two Multiaxis Thrust-Vectoring Nozzles at Mach Numbers up to 1.28," NASA TP-3313, May 1993.

[13]Burley, J. R., II, and Berrier, B. L., "Investigation of Installation Effects of Single-Engine Convergent-Divergent Nozzles," NASA TP-2078, Nov. 1982.

W. J. Devenport
Associate Editor